INSTITUTE OF PHYSICS PUBLISHING NANOTECHNOLOGY
Nanotechnology **16** (2005) 1238–1244 doi:10.1088/0957-4484/16/8/043

Patterning and fusion of CuO nanorods with a focused laser beam

Ting Yu[1], Chorng-Haur Sow[1,2], Aditya Gantimahapatruni[1], Fook-Chiong Cheong[1], Yanwu Zhu[1,2], Kok-Chung Chin[2], Xiaojing Xu[2], Chwee-Teck Lim[2,3], Zexiang Shen[1], John Thiam-Leong Thong[2,4] and Andrew Thye-Shen Wee[1,2]

[1] Department of Physics, Blk S12, Faculty of Science, National University of Singapore, 2 Science Drive 3, 117542, Singapore
[2] National University of Singapore Nanoscience and Nanotechnology Initiative, Singapore
[3] Department of Mechanical Engineering, National University of Singapore, 9 Engineering Drive 1, 117576, Singapore
[4] Department of Electrical and Computer Engineering, Faculty of Engineering, National University of Singapore, 4 Engineering Drive 3, 117576, Singapore

E-mail: physowch@nus.edu.sg

Received 3 January 2005, in final form 18 March 2005
Published 3 June 2005
Online at stacks.iop.org/Nano/16/1238

Abstract
We report a simple technique that facilitates the micropatterning of an aligned array of CuO nanorods on a substrate as well as the fusion of the nanorods into fused junctions. The technique utilizes a focused laser beam from a He–Ne laser with moderate power to melt away the pointed end of as-grown CuO nanorods resulting in the formation of microballs at the tips of the truncated nanorods. The size of the microballs and the length of the truncated CuO nanorods were found to be dependent on the laser power used during the process. The nature of the microballs formed was investigated by high-resolution transmission electron microscopy and Raman spectroscopy. Such a focused beam provides an effective means to modify the morphology of the as-grown nanorod array and to pattern the aligned CuO nanorod array into interesting and potentially useful configurations. In addition, the focused laser beam was utilized to fuse and join nanorods, which could potentially be useful in the fabrication of nanorod circuits and network repair.

(Some figures in this article are in colour only in the electronic version)

M This article features online multimedia enhancements

1. Introduction

One-dimensional (1D) nanomaterials have attracted much attention because of their unique and fascinating properties arising from their nanoscale dimensions [1]. The wealth of interesting behaviours renders these nanomaterials potentially useful building blocks for nanoscale devices [2–4]. In recent years, great progress has been made in the fabrication of 1D nanostructures [1]. Nanostructures made from a wide variety of materials have been reported [1]. In addition to novel routes for synthesis, it is also challenging to develop useful methods for creating patterns made from these nanomaterials. Such capabilities would be much valuable in the fabrication of useful devices, e.g. sensors [5], optoelectronics [6] and field emission devices [7, 8]. Extensive efforts focused on the development of techniques for creating nanostructures with unique but controlled configurations or patterns. These techniques include: (i) using patterned catalysts to define patterned arrays of the nanostructures [9]; (ii) utilizing structured templates like anodized alumina oxide from which patterned nanowires arise [10]; (iii) employing structured substrates from which the nanomaterials grow [11]; (iv) making use of fluidic assisted assembly to help define a network of nanowires [12]; and (v) fabricating nanopores on semiconductor substrates by electrochemical methods [13].

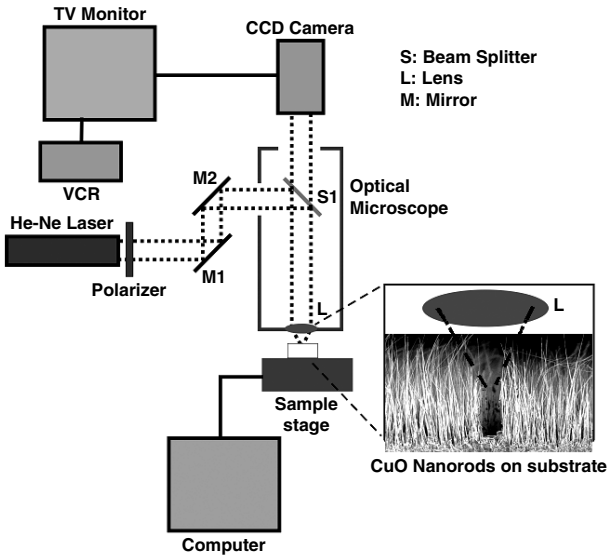

Figure 1. Schematic diagram of a simple focused laser beam system used in this work.

In this work, we present a simple method for creating micropatterns from aligned arrays of CuO nanorods on a substrate as well as for fusing the nanorods together into junctions. The technique utilizes a focused laser beam to induce patterns on thin film samples [14] as it readily melts away the pointed ends of as-grown CuO nanorods. The laser pruning resulted in the formation of submicron-sized balls (microballs) at the tips of the truncated nanorods. High-resolution transmission electron microscopy and Raman spectroscopy were employed to investigate the nature of the microballs formed. Such a focused beam provides an effective means to alter the morphology of the as-grown nanorod array and to pattern an aligned CuO nanorod array into potentially useful configurations. Moreover, the focused laser beam was utilized to fuse and connect nanorods together. This paper builds upon our earlier report [15] on the use of focused laser beams to trim and fabricate unique microstructures from aligned arrays of carbon nanotubes. The advantages of this technique are that it is simple and relatively inexpensive to implement.

2. Experimental details

Sample films with oriented CuO nanorods were prepared in an ambient atmosphere using a simple vapour–solid reaction method [16, 17]. Typically the substrates were copper plates (99.999% purity, Sigma-Aldrich Pte Ltd) with thickness of 0.5 cm and dimensions of about 10 cm × 3 cm. Before growth, the Cu plates were polished with sandpaper (320 grits), rinsed with deionized water and dried. The Cu plates were then heated on a hotplate in ambient conditions. The growth temperature was about 390–430 °C and the growth time varied from one day to three days. After cooling, a black layer was observed to form on the substrate. This layer was peeled off carefully and attached onto a silicon substrate with conducting tape before additional experiments were conducted. The morphologies of as-grown and laser-trimmed samples were studied by field

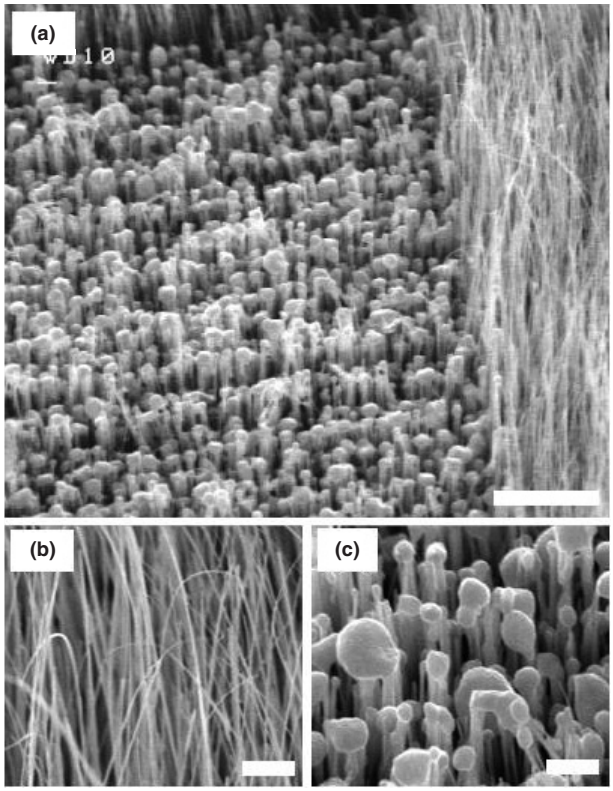

Figure 2. Oblique-view SEM images showing: (a) both as-grown and laser-trimmed parts of the CuO nanorod array; close-up views of (b) the as-grown region and (c) the laser-trimmed region. Scale bars: (a) 10 μm; (b), (c) 2 μm.

emission scanning electron microscopy (FESEM, JEOL JSM-6400F) and transmission electron microscopy (TEM, JEOL JEM-2010F). The crystal structures of these two samples were studied by high-resolution transmission electron microscopy (HRTEM, JEOL JEM-2010F). In the preparation of the sample for HRTEM, some of the trimmed nanorods were scratched off the substrate onto a TEM Cu grid with a lacy carbon film for TEM.

Figure 1 shows the schematic diagram of an optical microscope-focused laser beam system used in this work. When the focused beam was incident on the sample, it caused localized melting of nanorods in ambience. By moving the sample with respect to the focused laser beam, patterns can be created on the aligned nanorod array. A He–Ne laser (Coherent) emitting at a maximum beam power of 39 mW and at a wavelength of $\lambda = 632.8$ nm was employed. A polarizer was inserted in the beam path to vary the power of the linearly polarized laser beam. The parallel laser beam was then directed into an upright optical microscope via two reflecting mirrors (M1 and M2). Inside the microscope, the beam was directed towards an objective lens via a beam splitter (S1). The laser beam was then focused by the objective lens (L) with a magnification of 50×, a numerical aperture of 0.55 and a long working distance of 8.7 mm. The size of the focused laser beam was about ∼1.5 μm. The power of the laser beam after passing through the objective lens was measured to be about 55% of the power of the beam after it passed through the polarizer. The samples were placed on a

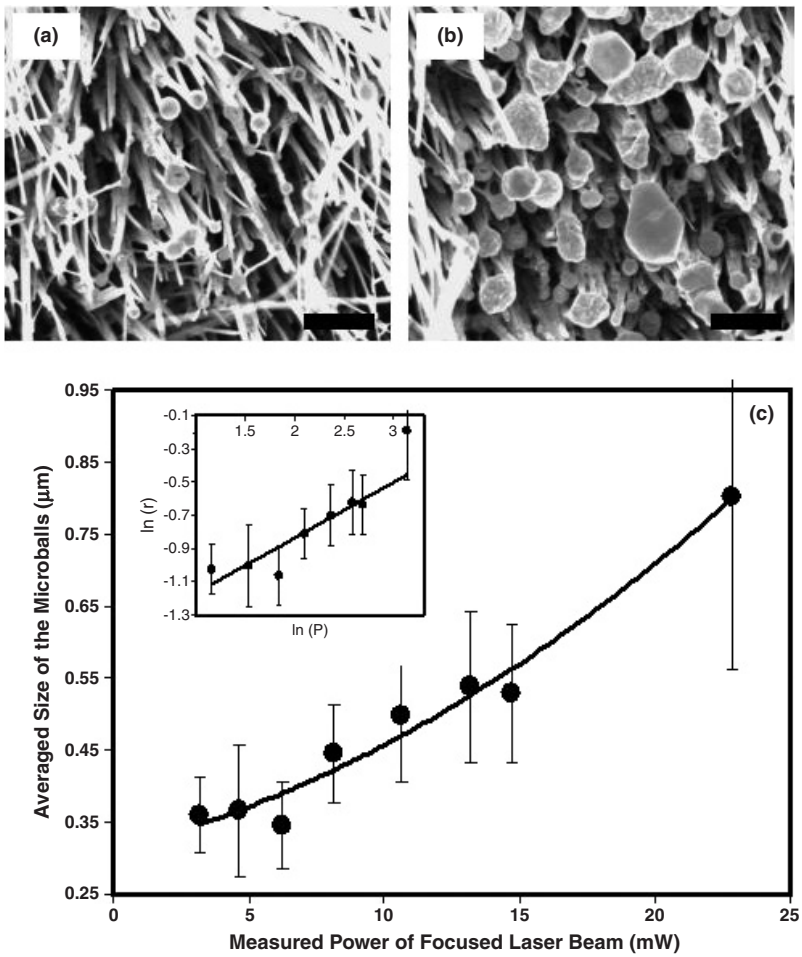

Figure 3. SEM images showing the formation of CuO nanorods with microballs at the tips as a result of laser trimming at (a) 8.2 mW, (b) 22.8 mW. Scale bars: 2 μm. (c) A plot of the average size of the microballs (r) versus the power of the laser beam (P) used. Inset: a plot of $\ln(r)$ versus $\ln(P)$ where a solid line with a gradient of $1/3$ is added.

computer-controlled, motorized stage (MICOS VT-80 System) with a minimum step size of 100 nm in the x–y direction. By moving the sample stage with respect to the focused beam, we were able to create nanorod patterns of the desired design. During the cutting of the nanorods, we can visually inspect the structures created simultaneously. The same objective lens (L) was used to collect light reflected from the sample for viewing purposes. A CCD camera was used to capture the images of the laser trimming process. The illumination of the sample was provided by an external Olympus LPGS light source (not shown in figure 1).

In order to perform the Raman scattering study on an isolated nanorod with a microball at the tip, a small piece of the laser-treated sample was submerged in de-ionized water and this was followed by 5 min of ultrasonic agitation. The nanorods (with microballs) became suspended in the deionized water. The suspension was dispersed and dried on a cover glass for Raman measurement. All micro-Raman spectra were measured in the backscattering geometry using a Renishaw Ramascope System 2000 with an Olympus microscope attachment. The 514 nm line of an argon-ion laser was used as the excitation source. To avoid laser fusing, the laser power was fixed at 2 mW during the Raman measurement. The spot size of the laser beam on the sample was about 700 nm in diameter.

3. Results and discussion

When a laser beam was focused on a sample film comprising an aligned array of CuO nanorods, it readily trimmed away the top layer of the film. Figure 2 shows a SEM image of a sample comprising both as-grown and laser-trimmed regions. When a focused laser beam was incident onto the CuO nanorods, the laser removed a fraction of the total length of the nanorod. We found that after laser trimming, the surface morphology of the film was populated with rounded microballs attached to the tip of one or more nanorods. These observations suggest the melting and re-solidification of CuO during and after focused laser irradiation respectively. Absorption of the laser beam by the CuO nanorods creates local heating resulting in melting of the upper segment of the CuO nanorods. The surface tension of the molten materials resulted in spherical microballs that subsequently cooled and solidified. As a result, the nanorods shortened with the appearance of these microballs. The melting temperature of bulk CuO is 1336 °C at 1 atm oxygen [18]. Laser-induced melting probably

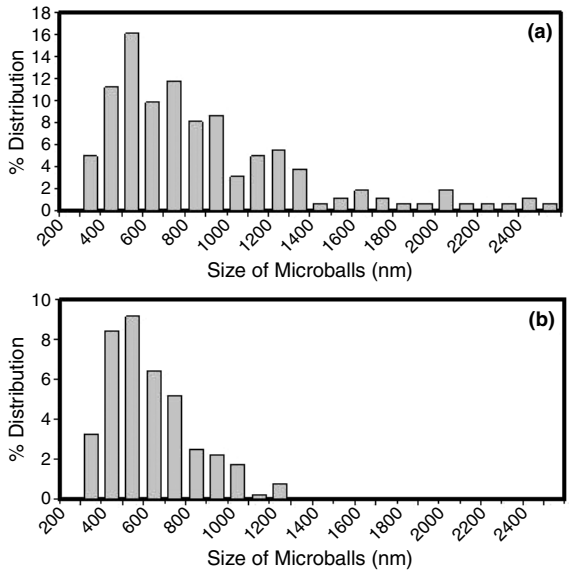

Figure 4. Distribution of the size of the CuO microballs formed as a result of laser pruning at powers of (a) 22.8 mW and (b) 13.1 mW.

occurs at lower temperatures since the melting temperature of nanosized material is typically lower than the bulk melting temperature due to the significance of surface energy of the low-dimensional system [19]. After laser trimming, the nanorod arrays became better aligned as compared with the as-grown region where the top part of the nanowires shows obvious bending (see figure 2(c)).

During the process of laser trimming, the power of the focused laser beam can be easily adjusted. In this way, one can investigate the difference in morphology of the laser-trimmed region as a function of the power of the focused laser beam. Figures 3(a), (b) show SEM images of the morphologies of the CuO nanorod array in a single channel created via laser pruning with measured laser powers of 8.2 and 22.8 mW respectively. Here the power of the laser corresponds to the measured laser power after the objective lens. Naturally, with higher laser power, more CuO material would be melted and this resulted in larger microballs when the molten CuO cooled. It is remarkable that only a small laser power was required to facilitate effective laser pruning of the CuO nanorods. Besides the concentration of the laser energy from the converging laser beam, effective absorption of the laser beam by the nanorods and poor thermal conductivity of the nanorods could be factors contributing to the effectiveness of the laser pruning. An as-grown sample typically consists of a high density of CuO nanowires. The focused laser beam typically affected a number of nanowires during the laser scan. Since some nanowires are in close proximity to each other, and in view of the presence of molten CuO material caused by the laser beam, it is common to find nanorods fused together capped with large microballs. The rounded microballs at the ends of the fused nanorods are clearly visible in the laser-pruned regions. From the measurements of the size (r) of the microballs from the SEM images such as those shown in figures 3(a), (b), we obtained a plot of the average size of the microballs versus the measured laser power (P) as shown in figure 3(c). Assuming that there is no loss of CuO via vapour formation during the transformation

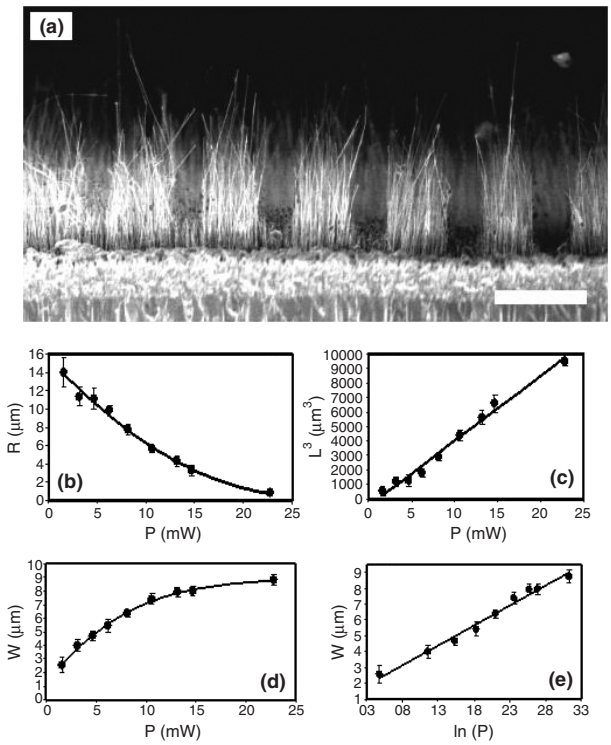

Figure 5. SEM images of the side view of the CuO nanorod array showing channels created by the laser trimming. The powers of the laser beam used, P, were (from right) 22.8, 14.7, 13.2, 10.6, 8.2, 6.3 mW. Scale bar: 20 μm. (b) A plot of the length of the remaining CuO nanorods, R, versus P. (c) A plot of the cube of the length of the CuO nanorods removed by the laser beam, L^3, versus P. (d) A plot of the width of the channels truncated, W, versus P. (e) A plot of W versus $\ln(P)$.

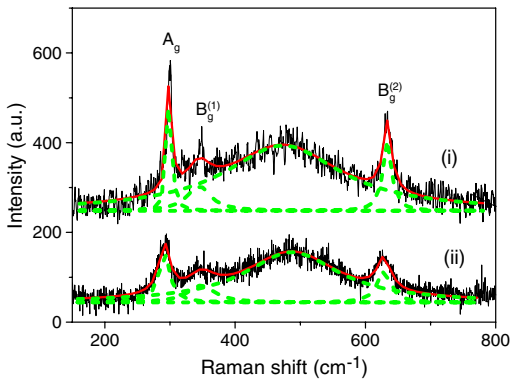

Figure 6. Raman spectra of the CuO (i) nanorods and (ii) microballs after laser pruning.

from nanorods to microballs, the laser energy absorbed by the nanorods is directly proportional to the mass of the melted materials, which for microball is in turn proportional to the cube of the size of the microballs. Hence $P \sim r^3$. The inset of figure 3(c) shows a plot of $\ln(r)$ versus $\ln(P)$ where a solid line with a gradient of $1/3$ was added to guide the eye. It should also be noted that at high laser power, the laser cut the nanorods all the way to their roots and the re-solidified CuO appeared to be more disc-like in shape. As a result, they have a larger apparent size from top-view SEM images.

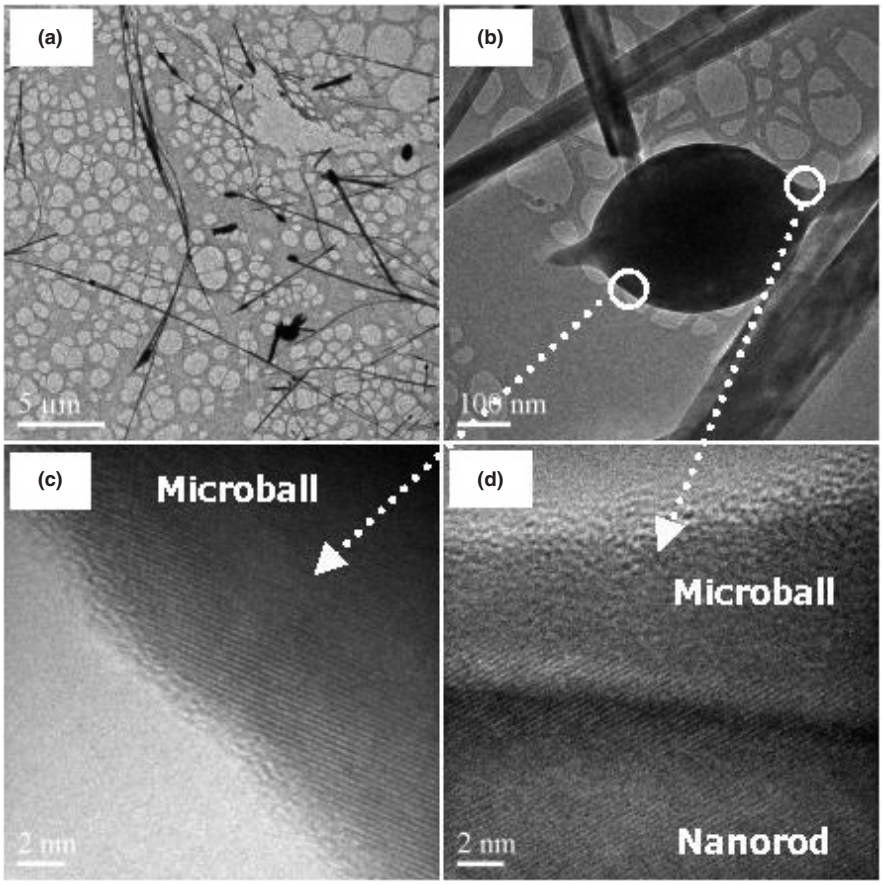

Figure 7. TEM images of (a) laser-trimmed CuO nanorods scattered on a Cu grid with a carbon film and (b) a microball. (c), (d) HRTEM images of the microball and nanorod indicated by the circles in (b).

Table 1. Fitting parameters for the Raman spectra of (i) CuO nanorods and (ii) microballs shown in figure 6.

	Panel (i)		Panel (ii)	
	Position (cm^{-1})	Linewidth (cm^{-1})	Position (cm^{-1})	Linewidth (cm^{-1})
A_g	298 ± 0.4	13 ± 0.2	294 ± 0.1	20 ± 0.3
$B_g^{(1)}$	347 ± 0.9	36 ± 0.2	347 ± 0.4	40 ± 0.9
$B_g^{(2)}$	633 ± 0.7	22 ± 0.9	628 ± 0.3	28 ± 0.9

From the SEM images, it was also clear that the size of the microballs has a broad distribution. Figure 4 shows the distribution of the size of the CuO microballs as a result of laser pruning at powers of (a) 22.8 mW and (b) 13.1 mW. A narrower size distribution was obtained using the lower laser power. The observed non-uniformity in the size of the microballs could be due to the intrinsic non-uniformity of the diameter of the as-grown nanorods and non-uniformity of heating in the focused area of the laser. With higher laser power, in addition to the above-mentioned contributions, one would expect that the fusion of adjacent nanorods would add on to the distribution and thus result in the broader size distribution of the microballs.

Varying the power of the focused laser beam could also control the length of the CuO nanorods and the width of the channel truncated by the beam. Figure 5(a) shows SEM images of the side view of a CuO nanorod array showing channels created by the laser trimming. The powers of the laser beam used were (from right) 22.8, 14.7, 13.2, 10.6, 8.2, 6.3 mW. It should be noted that these channels were created by laser pruning with one single laser scan. Figure 5(b) shows the trend of the length of the remaining nanorods, R, versus the power of the laser beam, P. The average length of the as-grown CuO nanorods in this sample was 22 ± 5 μm. It is evident that the length of the as-grown CuO nanorods is not uniform. However, this non-uniformity in the length of the nanorods could be improved with laser trimming. The length of the nanorod removed by the laser beam, L, can be obtained by taking the difference between the average as-grown length and R. A plot of L^3 versus P is shown in figure 5(c). The CuO nanorods generally have a shape with a narrow tip and a broad bottom (i.e. cone-like structure). That implies that more laser power is needed as one cuts deeper because of the greater mass of CuO to be melted. Integrating the mass of CuO nanorods

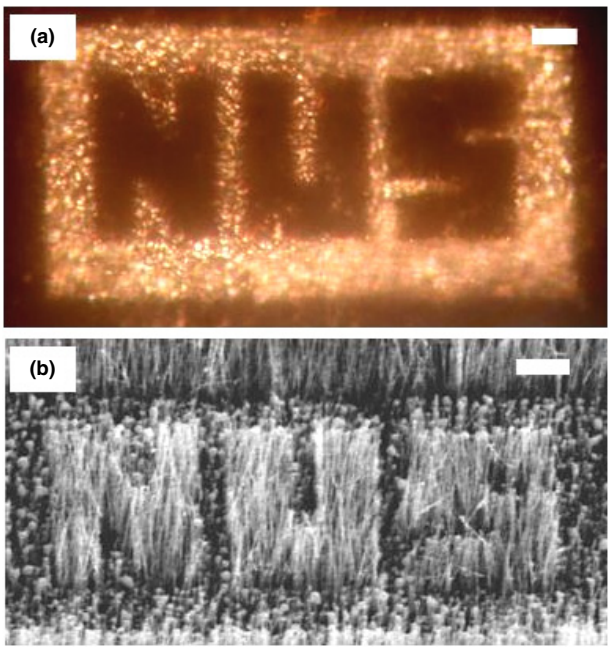

Figure 8. (a) Optical micrograph of letter formation created by laser cutting. (b) Oblique SEM view of the same patterned CuO nanorod array. Scale bars: 10 μm.

over the vertical length L suggests that the mass melted by the laser beam is proportional to L^3. And this is consistent with the observed linear relationship between L^3 and P as shown in figure 5(c). In addition to the length of the nanorods truncated by the laser beam, the width of the channel, W, created was also measured. A plot of W versus P is shown in figure 5(d) and we found an interesting linear relationship between W and $\ln(P)$ as shown in figure 5(e). The width of the channel truncated depends on the focused beam profile and the Gaussian intensity profile of the laser beam; in addition, more energy is required as the laser beam cuts deeper into the sample.

Figure 6 shows Raman spectra of the CuO nanorods and microballs after laser trimming (laser power: 5 mW). Since the cylindrical body of a nanorod and the microball at its tip can be readily identified under an optical microscope, one can selectively focus the laser beam on the microballs or nanorods independently and record their Raman spectra. Both of the Raman spectra as shown in figure 6 correspond to that of crystalline CuO [20]. This indicates that the microballs formed after laser trimming consist predominantly of CuO rather than Cu_2O, which was observed in the reduction of CuO by laser irradiation [21]. However, the parameters, i.e. linewidths and positions of Raman peaks, show obvious differences between nanorod and microball spectra. As shown in table 1, the linewidths of all the Raman peaks in spectrum (ii) are larger than those in spectrum (i). This broadening of the Raman peaks suggests that laser trimming could result in amorphous and/or polycrystalline phases in the microballs [22]. In addition, a red-shift of the Raman peaks in spectrum (ii) is present. This could to be due to the introduction of stress during the formation of microballs [23]. The humps centred at $\sim$480 cm^{-1} in the spectra were due to the cover-glass substrate. It should also be noted that we did not observe significant laser trimming or shape transformation during Raman spectroscopy due to the low laser power used during the experiments.

Figures 7(a) and (b) show TEM images of some laser-trimmed CuO nanorods scattered over a Cu grid with a carbon film. The microballs created by the laser trimming are clearly visible. Figures 7(c), (d) show HRTEM images of the tip of a microball and the nanorod–microball interface respectively. The spacing of the lattice (figures 7(c) and (d)) was measured to be 0.26 nm, corresponding to the lattice distance of the CuO monoclinic ($\bar{1}11$) crystal plane [24]. This indicates that the crystalline region of the microballs is still pure CuO. On the other hand, some regions (figure 7(d)) of the microballs were observed to be amorphous. After focused laser irradiation, the rapid cooling resulted in re-solidification into the observed microball which is not completely crystalline.

A focused laser beam facilitates the localized truncation of CuO nanorod arrays as defined by the focused laser spot, $\sim$1.5 μm. Coupling it with a precision programmable sample stage, we can readily fabricate unique patterned arrays of CuO nanorods. Figure 8 shows an example of 'NUS' letter formation comprising CuO nanorod arrays left behind after controllably removing some of the as-grown CuO nanorod array with the focused laser beam. Figure 8(a) shows an optical micrograph of the letter formation whereas figure 8(b) shows an oblique SEM view of the same patterned CuO nanorod array. It is interesting to note the remarkable change in the optical properties of the nanorod array upon laser pruning. The as-grown CuO nanorod array appeared to be black under optical microscopy in the reflection mode. The laser-pruned region scattered light much better and appeared to be much brighter. The improved scattering of light could be due to the formation of microballs at the tips of nanorods. This change in the optical property is particularly useful as it allows us to visually examine the laser-trimmed pattern. Video clips of the laser trimming of the CuO nanorod array can be found in the multimedia files available at stacks.iop.org/Nano/16/1238. With this simple technique, we can: modify the surface morphology of the as-grown CuO nanorod array; fabricate a sample consisting of CuO with different but controlled lengths; pattern the nanorod array as a template to support growth of other materials; and pattern the nanorod array for optimum nanorod density for field emission.

In addition to effecting laser patterning, the focused laser beam can also serve as a localized welding tool for fusing the CuO nanorods. As a simple feasibility test, we carried out the following experiment: after growing the CuO nanorod array, a piece of the sample was immersed in a vial with deionized water. The vial was then subjected to ultrasonic excitation causing some nanorods to detach from the substrate and become suspended in the deionized water. A drop of the aqueous suspension with the nanorods was then placed on a Si substrate and left to dry. As the water receded, the nanorods were randomly deposited on the substrate with some crossed nanorods. The nanorods were visible under an optical microscope and the focused laser spot was brought onto the crossed nanorods. In this way, we were able to melt and fuse the cross nanorods. Figure 9 shows SEM images of some of the CuO nanorods fused together created using this method. A potential useful extension of this experiment is first arranging the nanorods into desirable configurations using the manipulation techniques—e.g. fluidic alignment [12], electric field alignment [25] and line optical tweezers [26]—and then fusing them together with the laser beam into possibly useful integrated networks.

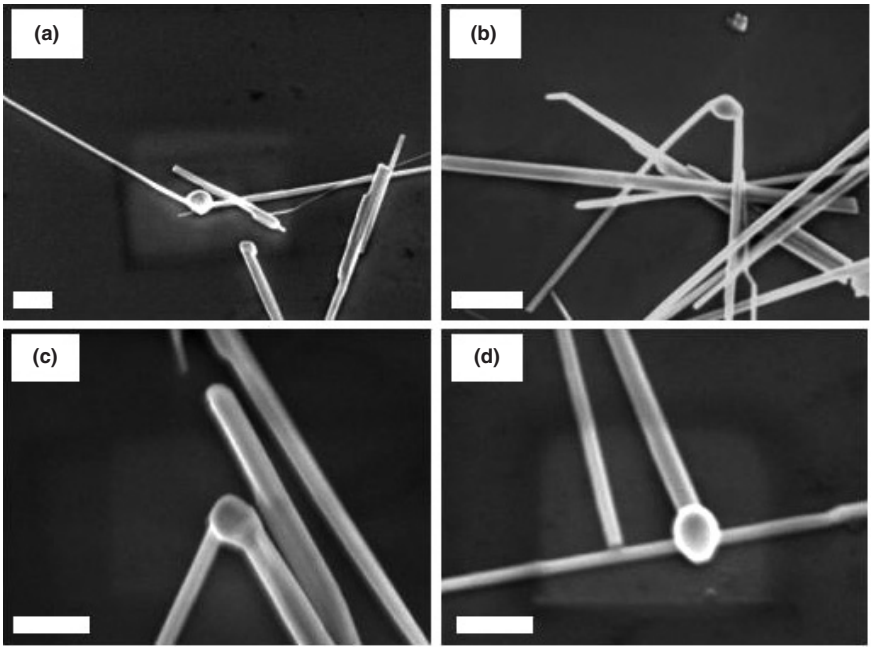

Figure 9. SEM images of CuO nanorods fused together created using the focused laser beam. Scale bars: (a), (b) 1 μm; (c), (d) 0.5 μm.

4. Conclusions

We report a simple technique that facilitates the micropatterning of aligned arrays of CuO nanorods on a substrate as well as the fusion of the nanorods into junctions. A focused laser beam provides an effective means of modifying the morphology of the as-grown nanorod array and patterning the aligned CuO nanorods into interesting and potentially useful configurations. The focused laser beam was also used to fuse and join nanorods. With further decrease of the focused laser spot size, this could be a simple method for joining CuO nanorods and could potentially be useful in the fabrication of nanorod networks.

Acknowledgments

TY acknowledges the support of Singapore Millennium Foundation. CHS acknowledges the support of National University of Singapore (NUS) and NUS Nanoscience and Nanotechnology Initiative.

References

[1] Xia Y N, Yang P D, Sun Y G, Wu Y Y, Mayers B, Gates B, Yin Y D, Kim F and Yan H Q 2003 *Adv. Mater.* **15** 353–89
[2] Cui Y, Björk M T, Liddle A, Sönnichsen C, Boussert B and Alivisatos A P 2004 *Nano Lett.* **6** 1093–8
[3] Wang Z L 2000 *Adv. Mater.* **12** 1295–8
[4] Hu J, Odom T W and Lieber C M 1999 *Acc. Chem. Res* **32** 435–45
[5] Soundarrajan P, Patil A and Dai L M 2003 *J. Vac. Sci. Technol.* A **21** 1198–201
[6] Chien F S S, Hsieh W F, Gwo S, Vladar A E and Dagata J A 2002 *J. Appl. Phys.* **91** 10044–50
[7] Oh S J, Zhang J, Cheng Y, Shimoda H and Zhou O 2004 *Appl. Phys. Lett.* **84** 3738–40
[8] Huang S M and Mau A W H 2003 *J. Phys. Chem.* B **107** 3455–8
[9] Wang X D, Summers C J and Wang Z L 2004 *Nano Lett.* **4** 423–6
[10] Xu H, Qin D H, Yang Z and Li H L 2003 *Mater. Chem. Phys.* **80** 524–8
[11] Martensson T, Borgstrom M, Seifert W, Ohlsson B J and Samuelson L 2003 *Nanotechnology* **14** 1255–8
[12] Huang Y, Duan X, Wei Q and Lieber C M 2001 *Science* **291** 630–3
[13] Foll H, Langa S, Cartensen J and Tiginyanu I M 2003 *Adv. Mater.* **15** 183–98
[14] Chauvy P F, Hoffmann P and Landolt D 2001 *Electrochem. Solid State Lett.* **4** C31–4
[15] Lim K Y, Sow C H, Lin J Y, Cheong F C, Shen Z X, Thong J T L, Chin K C and Wee A T S 2003 *Adv. Mater.* **15** 300–3
[16] Jiang X C, Herricks T and Xia Y N 2002 *Nano Lett.* **2** 1333–8
[17] Yu T, Zhao X, Shen Z X, Wu Y H and Su W H 2004 *J. Cryst. Growth* **268** 590–5
[18] http://www.webelements.com/webelements/compounds/text/Cu/Cu1O1-1317380.html
[19] Nanda K K, Sahu S N and Behera S N 2002 *Phys. Rev.* A **66** 013208–15
[20] Chen X K, Irwin J C and Franck J P 1995 *Phys. Rev.* B **52** R13130–3
[21] Sol C and Tilley R J D 2001 *J. Mater. Chem.* **11** 815–20
[22] Gotic M, Popovic S, Ivanda M and Music S 2003 *Mater. Lett.* **57** 3186–92
[23] Yu T, Tan S C, Shen Z X, Chen L W, Lin J Y and See A K 2002 *Appl. Phys. Lett.* **80** 2266
[24] *Joint Committee on Powder Diffraction Standards. Diffraction Data File, No. 45-0937. International Centre for Diffraction Data (ICDD, formerly JCPDS): Newtown Square, PA, 1991*
[25] Duan X F, Huang Y, Cui Y, Wang J F and Lieber C M 2001 *Nature* **409** 66–9
[26] Yu T, Cheong F C and Sow C H 2004 *Nanotechnology* **15** 1732